

The Role of Dielectric Relaxation in Charge Roller Performance

Ming-Kai Tse and Inan Chen

QEA, Inc.

99 South Bedford Street #4, Burlington, MA 01803 USA

Tel: (781) 221-0080 · Fax: (781) 221-7107

e-mail: info@qea.com

URL: www.qea.com

*Paper presented at the IS&T's NIP14
International Conference on Digital Printing Technologies
October 18-23, 1998, Toronto, Ontario, Canada*

The Role of Dielectric Relaxation in Charge Roller Performance

Ming-Kai Tse and Inan Chen***
QEA, Inc.
Burlington, Massachusetts/USA

Abstract

An innovative electrostatic charge decay (ECD) technique previously introduced has been shown to be a good predictor of charge roller performance. The physical reason behind the correlation between ECD and charging performance is that both processes depend on dielectric relaxation to rearrange the charge distribution in the resistive layer. In this paper, we present experimental and theoretical studies of dielectric relaxation in resistive materials used for charge rollers. It is shown that the process can be non-ohmic, and that information on charge injection and transport parameters in addition to resistivity is required for specifying an effective charge roller.

Introduction

A typical charge roller (CR) for electrophotographic copiers and printers consists of a layer of conductive elastomer coating on a metal shaft. In addition, a thinner and more resistive over-coating is generally applied to prevent destructive arcing to the photoreceptor (PR).¹ The electric and dielectric properties of the coatings can critically affect the uniformity and level of charging on a PR. In a previous paper, we introduced a non-contact and non-destructive measurement technique for CRs under conditions closely simulating the actual application of the device.² This electrostatic charge decay (ECD) technique has been shown to be a good predictor of CR performance. Direct measurements on PRs verify that CRs with faster rates of ECD produce higher surface potentials and better print quality. The physical reason behind the correlation between ECD and CR performance is that both processes depend on dielectric relaxation to rearrange the charge and voltage distributions in the layers. In this paper, we elucidate this correlation with a simple electrostatic model of roller charging. This is followed by discussion of experimental and theoretical studies of dielectric relaxation in resistive materials used in CRs. It is shown that the classical view of dielectric relaxation by RC circuit approximation does not always apply, and that additional information on charge injection and transport, as

revealed by the ECD measurements, is required for specifying an effective CR.

Electrostatic Model of Roller Charging

The physical mechanism of roller charging of the PR can be described with the one-dimensional geometry of a three-layer system, consisting of the grounded PR, the resistive coating of the charging roller and the air gap, shown in Fig. 1. All curvatures are neglected.

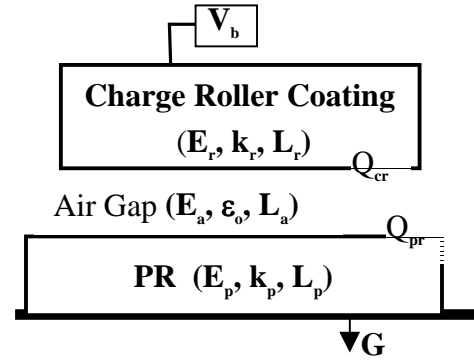


Figure 1. Schematic 1-D model of CR and PR system

The applied bias voltage V_b is divided into voltages across the PR V_p , the air gap V_a , and the roller coating V_r , as follows:

$$V_b = V_p + V_a + V_r = -E_p L_p - E_a L_a - E_r L_r \quad (1)$$

where E is the field and L is the layer thickness, with the subscripts p , a and r referring to PR, air gap and roller coating, respectively. The PR and air gap can be assumed to be space-charge free, and hence E_p and E_a are constant across the respective layers. In the electrostatic model, the coating on the roller is to be simulated by a perfect dielectric of various thicknesses, and hence the field E_r is also constant across the layer.

At the instant of bias application, the charge densities at the charge roller/air-gap interface Q_{cr} and at the air-gap/PR interface Q_{pr} are both zero. Using the Gauss theorem to eliminate the fields E_r and E_p , one obtains the initial air-gap voltage V_a as

$$V_a = -E_a L_a = V_b L_a / (D_p + L_a + D_r) \quad (2)$$

* Contact for inquiries

** Consulting scientist

where the D_s are the dielectric thicknesses, $D = L/k$, (with $k =$ dielectric constant). If the dielectric thickness of the roller layer D_r is much larger than the other two, L_a and D_p , most of the voltage drop is in this layer. In this case, the air-gap voltage V_a is likely to be smaller than the threshold voltage for air breakdown V_{th} .

For an air gap greater than $8 \mu\text{m}$, the air breakdown threshold voltage (at standard pressure and temperature) can be approximately represented by $V_{th}(L_a) = 312 + 6.2L_a$ (with L_a in μm and V_{th} in volts).³

The dashed line in Fig. 2 shows the above relationship between V_{th} and L_a (i.e. Paschen curve). Also shown in Fig. 2 are the initial air-gap voltages, Eq.(2), calculated for values of $D_r = 240, 150, 90, 60$ and $30 \mu\text{m}$ (for a dielectric constant $k_r = 2.5$, these correspond to $L_r = 600, 375, 225, 150$, and $75 \mu\text{m}$). The PR is assumed to have a dielectric thickness of $10 \mu\text{m}$ (e.g. with $k_p = 2.5$ and $L_p = 25 \mu\text{m}$), and the bias voltage is $V_b = 1200$ volts.

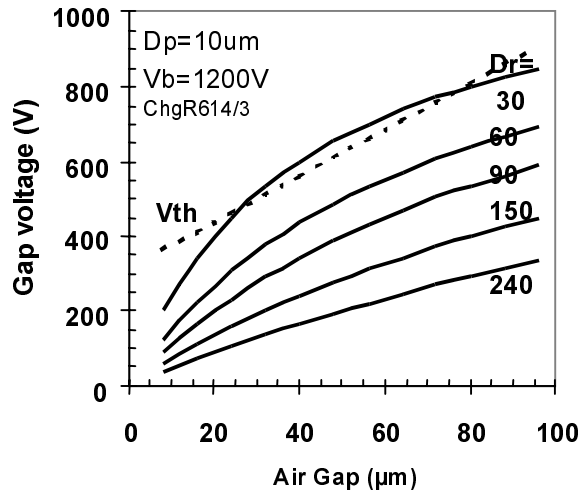


Figure 2. Air gap voltage vs. gap size L_a , calculated for various dielectric thicknesses D_r of the roller coating layer. The air breakdown threshold voltage V_{th} is shown by the dashed line (for $L_a > 8 \mu\text{m}$).

It can be seen that under these conditions, the air-gap voltage can exceed the threshold voltage only when the dielectric thickness of the roller coating is reduced to about $30 \mu\text{m}$. By collapsing the voltage across the layer, dielectric relaxation in the roller coating provides a process which effectively reduces the dielectric thickness of a layer with a fixed physical thickness.

In general, the roller coating consists of a thicker (a few mm) elastomer layer with a nominal conductivity $\sigma = 10^{-7}$ S/cm or higher, and a much thinner ($\approx 100 \mu\text{m}$) overcoat layer of a much lower nominal conductivity ($\sigma = 10^{-10}$ S/cm or less). The dielectric relaxation time (for details, see next section) of the elastomer layer is of the order of $\tau_r = \epsilon/\sigma \approx 1 \mu\text{sec}$, (where ϵ is the permittivity), and is about three orders of magnitude shorter than the dielectric relaxation time of the overcoat layer. Therefore, the voltage across the roller coating is essentially dominated by the voltage across the overcoat layer, in spite of the smaller thickness. The

dielectric relaxation in the overcoat layer is investigated in the following section.

Principle of Electrostatic Charge Decay (ECD)

In ECD measurements, the surface of a resistive layer on a grounded electrode (e.g. a CR) is corona charged to a voltage V_0 in a very short time (Fig. 3). The subsequent decay of the surface voltage V_s due to dielectric relaxation in the resistive layer is monitored by an electrostatic voltmeter.

In the classical treatment of dielectric relaxation, the sample is represented by a resistor R and a capacitor C in parallel, as shown in the lower part of Fig. 3. The equivalent circuit theory predicts that the surface voltage will decay exponentially, with a time constant τ , known as the "dielectric relaxation time,"

$$V(t) = V_0 \exp(-t/\tau), \quad \text{with } \tau = RC = \epsilon/\sigma \quad (3)$$

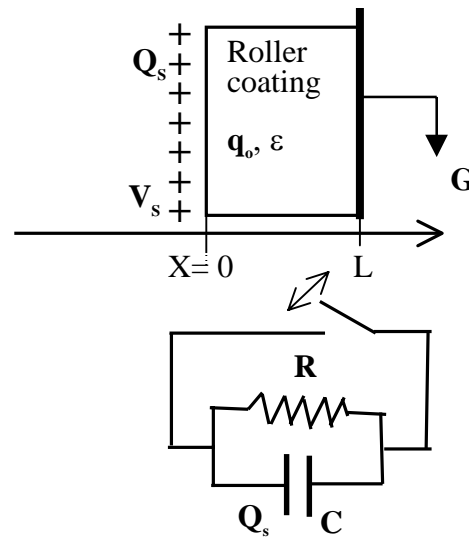


Figure 3. Schematic of ECD measurements, and the equivalent RC circuit.

In reality, however, a perfect exponential decay is seldom observed in materials commonly used for CR coating. Figure 4 shows representative ECD results obtained with three CRs. It is obvious from the semi-log plots that the voltage decay is not exponential, particularly as time increases. A linear extrapolation of the initial voltage decay shown in Fig. 4 gives an exponential decay with a time constant of the order of $\tau \approx 1$ sec, which corresponds to a conductivity of the order of $\sigma \approx 10^{-13}$ to 10^{-12} S/cm. This value is much smaller than that suggested by the suppliers. Even if this value is of the same order of magnitude as the one suggested, the actual voltage in the non-exponential tail (for $t > 1$ sec) can differ significantly from that expected from the RC model.

This discrepancy between the RC circuit theory and experimental observations arises because the electrical properties of the materials are specified only by resistance R and capacitance C , (or, equivalently, by permittivity ϵ and conductivity σ). In fact, in materials of present interest,

(classified as "semi-insulators"), the dielectric relaxation is controlled by three additional factors: (a) efficiency of charge injection from the surface and the substrate, (b) rate

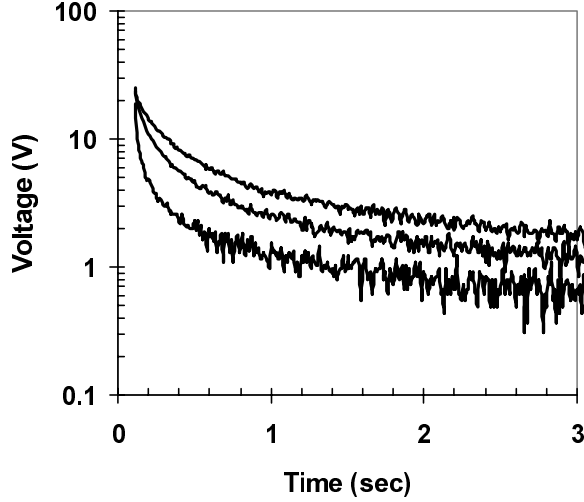


Figure 4. ECD experimental results on three representative CR.

of field induced charge generation in the bulk of the sample, and (c) mean life-time of charges before being trapped. The first two contribute to the voltage decay, while the last prevents the decay from being completed.

A complete treatment of dielectric relaxation applicable to semi-insulators starts with the expression of the total current J_T as the sum of conduction and displacement currents,

$$J_T = (\mu_p q_p + \mu_n q_n)E + \varepsilon(\partial E/\partial t) = 0 \quad (4)$$

where μ and q denote the charge mobility and density, respectively, with the subscripts p and n referring to positive and negative charge species, respectively. The total current vanishes because of the open circuit condition of ECD measurements. Noting that the integral of field E over the sample thickness L yields the surface voltage V_s , an integration of Eq.(4) gives the voltage decay rate as,

$$dV_s/dt = -(1/\varepsilon) \int_0^L (\mu_p q_p + \mu_n q_n) E dx \quad (5)$$

The time evolution of local charge densities, $q_p(x,t)$ and $q_n(x,t)$, can be calculated from the continuity equations:

$$\partial q_p/\partial t = -\partial(\mu_p q_p E)/\partial x + G(E) - q_p/\tau_p \quad (6)$$

and a similar equation for the negative charge density q_n . Here $G(E)$ represents the rate of field-induced charge generation, and τ_p and τ_n denote the mean life-time for positive and negative charges, respectively. The density of trapped charges q_t increases with time according to:

$$\partial q_t/\partial t = q_p/\tau_p + q_n/\tau_n \quad (7)$$

At any instant of time, the field E is governed by Poisson's equation, with the boundary condition that the surface field is, $E(0) = Q_s/\varepsilon$.

The injection of charge from the surface and the substrate can be specified by the expressions for the

conduction currents $J_p(0)$ at $x = 0$, and $J_n(L)$ at $x = L$. For example, it is conceivable that these currents depend linearly on the fields at $x = 0$ and $x = L$, respectively; then,

$$J_p(0) = s_0 E(0); \quad J_n(L) = s_1 E(L) \quad (8)$$

where s_0 and s_1 are the proportionality constants which have the same dimension as conductivity.

The above set of equations can be solved by numerical iteration, starting with the initial conditions that:

$$\begin{aligned} E(x, 0) &= E_0 = V_0/L; \quad Q_s(0) = \varepsilon E_0; \\ q_p(x, 0) &= -q_n(x, 0) = q_e; \quad q_t(x, 0) = 0. \end{aligned} \quad (9)$$

where q_e denotes the free charge density at equilibrium, with which the sample conductivity σ is given by, $\sigma = (\mu_p + \mu_n)q_e$.

The typical values of various parameters in materials of present interest are listed below.

$$\begin{aligned} \varepsilon &\approx 2 \times 10^{-13} \text{ f/cm}; \quad L \approx 10^2 \text{ cm} \\ \therefore C &= \varepsilon/L \approx 2 \times 10^{-11} \text{ f/cm} \\ \sigma &\approx 10^{-10} \text{ S/cm}; \quad \mu \approx 10^4 \text{ cm}^2/\text{V-sec} \\ \therefore q_e &= \sigma/2\mu \approx 5 \times 10^7 \text{ coul/cm}^3 \\ V_0 &\approx 100 \text{ V}; \quad E_0 = V_0/L \approx 10^4 \text{ V/cm} \\ \therefore Q_{s0} &= \varepsilon E_0 \approx 2 \times 10^9 \text{ coul/cm}^2 \end{aligned} \quad (10)$$

With these typical values, the layer density of charge at equilibrium is of the same order of magnitude as (or greater than) the initial surface charge density Q_{s0} :

$$Q_e = q_e L \approx 5 \times 10^9 \text{ coul/cm}^2 \gg Q_{s0} \quad (11)$$

Similarly, the nominal transit time, (i.e. the time required for a charge to transit the layer at the initial field E_0), defined by,

$$t_0 = L/\mu E_0 \approx 10^2 \text{ sec} \gg \tau_r \quad (12)$$

is of the same order of magnitude as (or longer than) the dielectric relaxation time $\tau_r = \varepsilon/\sigma \approx 2 \times 10^3 \text{ sec}$. These two conditions, $Q_e \geq Q_{s0}$ and $t_0 \geq \tau_r$, are the characteristic features of dielectric relaxation in semi-insulators.

In the following, representative numerical results of dielectric relaxation in semi-insulators, which demonstrate the deviations from the exponential decay, Eq.(3), are presented and discussed.

Figure 5 shows the calculated voltage decay with time, for the case of $Q_e = Q_{s0}$, with various injection rates. The voltage is given in units of the initial value V_0 , and the time in units of the nominal transit time t_0 defined by Eq.(12). It is assumed that the mobilities of positive and negative charges are equal, and that the field-induced generation and trapping are negligible. The injections from the two boundaries are assumed to be symmetrical, and the parameter values, $s_0 = s_1$, are varied from 0 to 10, in units of $[\varepsilon \mu V_0/L^2]$ ($\approx 2 \times 10^{-11}$ amp/Vsec). The physical meaning of this unit value will be clear from the features of the decay curves discussed below.

It can be seen that an exponential decay with a time constant τ_r ($= t_0/2$, in this example), predicted by Eq.(3), is realized only when the injection parameter is $s_0 = s_1 = 1$. For

charge injection less than this rate, the decay is slower than exponential. The electrode contacts that can provide the unit injection rate are commonly referred to as "Ohmic contacts".

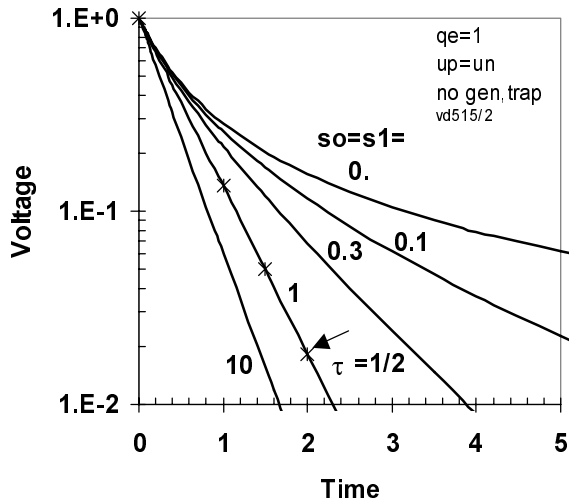


Figure 5. Voltage decay by symmetric injection.

In fact, the injection is unlikely to be symmetrical in the cases of present interest, because the two boundaries are in contact with different media (virtual electrode with corona charged surface at $x=0$ and conductive elastomer/metal electrode at $x=L$). This introduces another cause for non-exponential decay as shown in Fig. 6. In Fig. 6, the parameter for injection from the (corona charged) surface is assumed to have a small value, $s_0 = 0.1$, and the parameter for injection from the (conductive) substrate s_1 is varied. The other parameter values are identical to those of Fig. 5. It can be seen that with this weak injection at one contact, the decay can never be exponential (the dashed line) as given by Eq.(3).

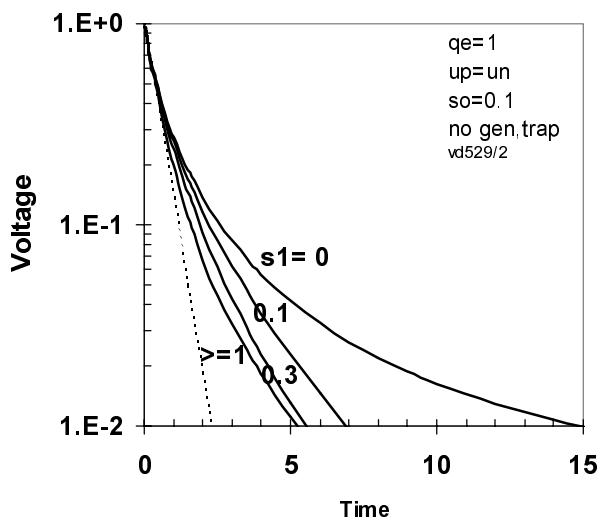


Figure 6. Voltage decay for asymmetric injection.

The consequences of limited charge life-time ($\tau_p, \tau_n < \infty$) are illustrated in Fig. 7. Even with both contacts being Ohmic ($s_0 = s_1 = 1$), the curves show that the decay cannot be exponential unless the life time is $\tau_p = \tau_n > 10t_0$. A distinct feature of trap-limited decay is that for $\tau_p = \tau_n < t_0$, the voltage decays to a quasi-steady (residual) value in a few transit times t_0 . The residual voltage increases as the life-time decreases.

Similar V-t plots can be obtained for the case of voltage decay caused by field induced charge generation. They are not included here because the mechanism is less likely to be operative in CRs.

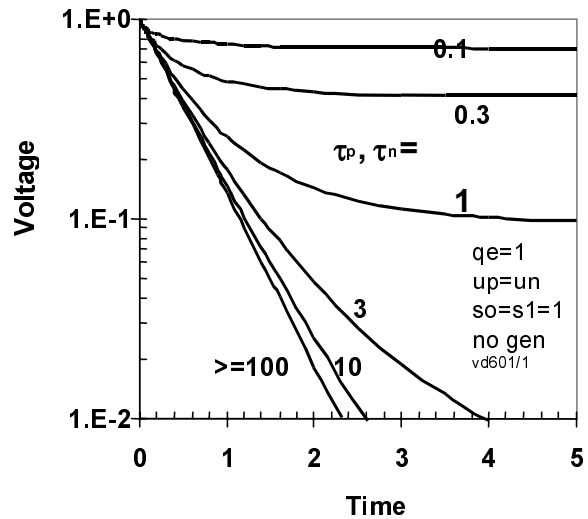


Figure 7. Voltage decay with limited charge life-times τ_p, τ_n (in units of t_0)

Conclusions

The experimental ECD data in Fig. 4 show that, in general, the voltage decay in CR coating does not follow the exponential time dependence. The results of the numerical simulations shown in Figs. 5-7 demonstrate that this deviation from the prediction of the RC equivalent circuit theory can be accounted for either by different degrees of charge injection or by charge life time, or by a combination of the two. Although a unique determination of the extent of each mechanism is not easy, it is clear that the traditional specification of the electrical property of the coating by its conductivity (or resistivity) is not sufficient to predict dielectric relaxation, and hence, CR performance. On the other hand, the ECD technique and the associated automated test equipment² can provide an efficient and physically significant evaluation of CR performance.

References

1. H. Tanaka and M.Okunuki, US Patent 5,089,851 (1992)
2. M. K. Tse, D. J. Forrest, and F. Y. Wong, "Predicting charge roller performance in electrophotography using electrostatic charge decay measurements", *IS&T NIP11*, P.383 (1995)

3. R. M. Schaffert, *Electrophotography*, The Focal Press, (1975) p.523.
4. I. Chen, J. Mort, M. A. Machonkin, J. R. Larson, and F. Bonsignore, *J. Appl. Phys.* **80**, 6796 (1996)

Biography

Dr. Ming-Kai Tse founded QEA, Inc. in 1987. The company designs and manufactures automated quality

control test systems for manufacturing and R&D applications in digital printing. Dr. Tse was a professor of Mechanical Engineering at the Massachusetts Institute of Technology between 1982 and 1989. At MIT he specialized in the areas of manufacturing, non-destructive testing, and quality engineering. Dr. Tse received his BS degree in Mechanical Engineering from Cornell University and his MS and PhD degrees, both in Mechanical Engineering, from MIT.